LA-UR-96- 2318

CONF-961017--3

Title: Resonant Ultrasound Spectroscopy

Author(s):
F. Chu, CMS
D. J. Thoma, MST-6
Y. He, CMS
S. A. Maloy, MST-4
T. E. Mitchell, CMS

Submitted to:
1996 TMS Meeting
Cincinatti, Ohio
October 6-10, 1996

Los Alamos
NATIONAL LABORATORY

Form No. 836 R5
ST 2629 10/91

DISCLAIMER

RESONANT ULTRASOUND SPECTROSCOPY: ELASTIC PROPERTIES OF SOME IMTERMETALLIC COMPOUNDS

F. Chu, D. J. Thoma, Y. He, S. A. Maloy, and T. E. Mitchell

Materials Science Technology Division, Mail Stop K 765

Los Alamos National Laboratory, Los Alamos, NM, 87545, U. S. A.

Abstract

A novel nondestructive evaluation method, resonant ultrasound spectroscopy (RUS), is reviewed with an emphasis upon defining the elastic properties of intermetallic phases. The applications and advantages of RUS as compared to other conventional elastic constant measurement methods are explained. RUS has been employed to measure the elastic properties of single crystal and/or polycrystalline intermetallics, such as Laves phases (C15 HfV_2 and $NbCr_2$), Nb-modified titanium aluminides, and transition metal disilicides ($C11_b$ $MoSi_2$, C40 $NbSi_2$ and $TaSi_2$). For Laves phases, the elastic properties of HfV_2-based C15 phases show various anomalies and those of C15 $NbCr_2$ do not. For Nb-modified titanium aluminides, the elastic properties of O-phase alloys are investigated as a function of alloying content. For transition metal disilicides, single crystal elastic constants of $MoSi_2$, $NbSi_2$, and $TaSi_2$ are obtained and compared. Based on the experimentally determined elastic properties, the characteristics of interatomic bonding in these materials are examined and the possible impact of the elastic properties on mechanical behavior is discussed.

Introduction

In recent years, various nondestructive evaluation (NDE) methods have been developed and applied to study materials properties. In this paper, we present a novel nondestructive evaluation method, resonant ultrasound spectroscopy (RUS) (1-4), with an emphasis upon defining the elastic properties of high temperature structural intermetallic alloys.

Resonant Ultrasound Spectroscopy

The elastic constants of a material can be determined in different ways. In nondestructive evaluation, conventional pulse-echo method and resonant ultrasound spectroscopy are two typical tools for measuring the elastic properties of a solid material. The resonant ultrasound spectroscopy technique was originally developed by Fraser and LeCraw (5) and improved by Soga and Anderson (6) for small isotropic spheres. Later, Demarest (7) applied this technique to an isotropic specimen with a cube shape. Ohno (8) further extended this method to a rectangular parallelepiped specimen with orthorhombic symmetry. Compared with conventional ultrasonic methods for measuring elastic constants, RUS offers several advantages. First, many specimen geometries are usable, such as sphere, cylinder, and parallelepiped. Second, measurements can be made on a small specimen with size less than 1 mm, which is important for materials where only small monocrystals are available. Third, all independent elastic constants c_{ij} can be determined simultaneously with one measurement. Fourth, for difficult-to-orient crystals, the crystallographic orientations can also be determined together with their elastic constants from resonance spectra. Most importantly, RUS results are more accurate than those obtained by measuring velocities of ultrasonic waves along different crystal orientations. In the traditional ultrasonic velocity measurement method, the small sample dimensions make it difficult to measure the sound velocity accurately, which may induce some error. More seriously, low crystal symmetry poses another intrinsic problem (9): the c_{ij} are found in the solution of Christoffel equation using the phase velocity (V_p) of the elastic waves along various directions (10). However, since the elastic pulses propagate at a group velocity (V_g) in the medium, it is V_g that is measured in the pulse-echo method, and V_g coincides with V_p only along the symmetry axes (10). For crystals with high symmetry (e.g. cubic) c_{ij} can be easily determined by measuring the V_g (V_p) along the principal crystal axes, but for crystals with lower symmetry, one has to measure V_g in some non-principal symmetry directions, along

which V_g and V_p are neither collinear nor the same in magnitude. Therefore, it is easy to measure the diagonal elastic constants (c_{ii}) using the pulse-echo method, since they can be determined from V_g (V_p) of the pure longitudinal and transverse (shear) waves propagating along principal axes. To obtain the mixed-index c_{ij} ($i \neq j$), one has to measure the V_g of either quasi-longitudinal or quasi-transverse modes propagating along several arbitrary directions, which induces intrinsic errors to the off-diagonal c_{ij}. However, RUS has no such intrinsic problem. Recent work on $MoSi_2$ single crystals shows that c_{ii} obtained from RUS and the ultrasonic velocity measurement are basically the same (within 1~2% error) and the c_{ij} ($i \neq j$) obtained from RUS are more accurate than those obtained from the ultrasonic velocity measurement (9). Because of the recent enhancements of RUS, this method has been successfully used to determine the elastic constants of various kinds of solid materials, especially high temperature structural intermetallic alloys, such as Laves phases (11, 12), titanium aluminides (13-14), and transition metal disilicides (15-16).

Figure 1 shows a schematic diagram of the measurement setup. The parallelepiped specimen is mounted between two $LiNbO_3$-diamond-composite piezoelectric transducers with the two corners on a body diagonal of the specimen touching the transducers.

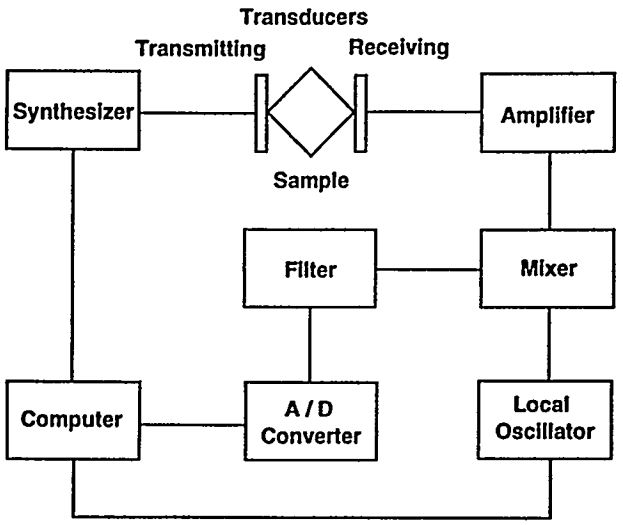

Figure 1: Schematic diagram of the measurement setup for resonant ultrasound spectroscopy.

A general RUS measurement (1, 2, 3, 16) determines the natural frequencies of a solid specimen with stress-free boundary conditions by measuring the resonance frequencies of the specimen when it is held lightly without bonding agents at two corners between two transducers. One transducer drives vibrations in the specimen at a tunable frequency. The other measures the frequency of the specimen's response. As the frequency of the drive is swept, a set of resonant frequencies is recorded. The positions of the resonant peaks occur at the natural frequencies can be used to determine the elastic constants of the specimen, based on the physics and mathematics presented in (1, 17).

Using the method developed by Demarest (7), Ohno (8), Visscher (18), Migliori et al. (1), and Maynard (17), we can easily calculate resonant frequencies of a solid from its elastic constants, dimensions, and mass density. Since no analytic method exists, we have to solve the inverse problem numerically to determine elastic constants from resonant frequencies in the following way.

First, we estimate the elastic constants as closely as possible from other sources (for example, using the weighted average values based on the rule of mixtures). Then we calculate the resonant frequencies using the estimated elastic constants, the dimensions and the mass density of the specimen.

Second, we define a figure of merit:

$$F = \sum_{i=1}^{N} \omega_i (f_i - g_i)^2 \qquad (1)$$

Here, g_i and f_i indicate the i-th measured and calculated frequencies, respectively; N denotes the total number of measured frequencies; and ω_i is a weighting factor chosen (usually either 0 or $1/g_i^2$, so that F is a measure of fractional deviation) to reflect the degree of confidence in the measured frequency g_i.

Finally, we use the Levenberg-Marquardt method (19) as a systematic scheme to locate the minimum of F in a multidimensional elastic-constant space. We estimate the accuracy of the elastic constants c_{ij} by considering the shape of the surface F near the minimum. F is assumed to be a quadratic function of the elastic constants in this neighborhood, so that the surfaces of constant F are ellipsoid with major axes related to the accuracy with which the corresponding elastic constants are determined. We estimate the accuracy for each c_{ij} by finding the length of the corresponding semi-major axis of the ellipsoid when F exceeds the minimum by 2%.

Using the above method, we can measure the elastic parameters of single crystalline and polycrystalline materials in the following way. For single crystal materials, the specimen is sectioned along major crystallographic axes. Independent elastic constants

of the system, c_{ij}, can be obtained by fitting the experimentally measured RUS spectrum. Using the elastic stiffness constants matrix, the elastic compliance constant matrix can be obtained. Furthermore, the isotropic elastic moduli and the Poisson's ratio of the system can be calculated using the elastic stiffness constants, c_{ij}, and compliance constants, s_{ij}, based on the Voigt, Reuss, and Hill averages (20).

For a polycrystalline material, due to its isotropic symmetry, the two independent c_{ij} are usually chosen to be c_{11} and c_{44}. Using the following relationship, we obtain four isotropic elastic parameters from its c_{11} and c_{44}:

Shear modulus: $$G = c_{44}, \quad (2)$$

Young's modulus: $$E = \frac{c_{44}(3c_{11} - 4c_{44})}{c_{11} - c_{44}}, \quad (3)$$

Bulk modulus: $$B = \frac{1}{3}(3c_{11} - 4c_{44}), \quad (4)$$

Poisson's ratio: $$\nu = \frac{1}{2}\frac{c_{11} - 2c_{44}}{c_{11} - c_{44}}. \quad (5)$$

In addition, in order to verify the texture dependence of the measurements, i.e., the extent to which the alloy is isotropic, we can fit the experimental resonances by two different schemes: isotropic fitting and orthorhombic fitting. In the isotropic fitting, we assume the specimen is homogenous and isotropic without any texture. In the orthorhombic fitting, we assume an orthorhombic symmetry, which allows all nine c_{ij} considered to change independently. The comparison of the isotropic moduli and the Poisson's ratio obtained from the two fittings shows the texture of the polycrystalline material.

Applications of RUS

The positions of the peaks occur at the natural frequencies f_n (from which the elastic parameters are determined), and the quality factor (Q, given by f_n divided by the full width of a peak at its half-power points) for each resonance provide information about the dissipation of elastic energy in the solid. Based on this principle, RUS has been extensively used in various kinds of scientific fields, e.g., in geophysics for the measurement of thermodynamic properties and anharmonic effects of materials, and in studies of quasicrystals (21).

The most important application of RUS is obviously the measurement of elastic properties of solid materials. In this paper, we summarize our work on defining the elastic parameters of high temperature structural intermetallic phases.

Because of growing interest in intermetallic compounds as potential high temperature structural materials, there have been many investigations carried out on various compounds, mostly structures that are ordered forms of simple fcc, bcc and hcp metals, e.g., Ni_3Al and NiAl. The elastic properties of these alloys have been well defined. If new intermetallic-based alloys are to be selected on the basis of low density and high melting temperature, as would be required for use in rotating components in the hot sections of gas turbines, for example, then the attraction of three groups of materials immediately becomes apparent: topologically close packed (TCP) compounds, titanium aluminides, and silicide-based compounds.

In the group of TCP intermetallics, the Laves phases constitute the single largest group. A number of these phases have quite high melting temperatures, low densities and high oxidation resistance. Among them, two cubic Laves phases, $NbCr_2$ (22) and HfV_2 (23, 24) have been subject to the study of physical metallurgy and mechanical properties.

In titanium aluminides, TiAl and Ti_3Al have been studied for a long time as high temperature structural materials. Recently, Nb-modified Ti_3Al, O-phase in Ti-Al-Nb alloys is found particularly interesting because of its excellent mechanical properties (25, 26).

For silicide-based alloys, transition metal disilicides have been attractive as potential high temperature structural materials. Among them, transition metal disilicides, e.g., $C11_b$ $MoSi_2$, and C40 $NbSi_2$ and $TaSi_2$, have been studied extensively (27, 28, 29, 30).

However, the elastic properties of all these intermetallic alloys have not been studied comprehensively. Elastic properties of a solid are important because they relate to various fundamental solid-state phenomena such as interatomic potentials, equations of state, and phonon spectra. Elastic properties are also linked thermodynamically with specific heat, thermal expansion, Debye temperature, and Gruneisen parameter. Most important, knowledge of elastic constants is essential for many practical applications related to the mechanical properties of a solid as well: load-deflection, thermoelastic stress, internal strain (residual stress), sound velocities, fracture toughness and dislocation core structure, etc.

Elastic Properties of Laves Phases

We have defined the isotropic elastic properties of C15 $NbCr_2$ and HfV_2+Nb polycrystals.

$NbCr_2$

Arc-melted buttons of C15 $NbCr_2$ were made in an argon atmosphere using elemental Nb and Cr with nominal purities of 99.99 at.% and 99.9 at.%, respectively. The buttons were turned over and remelted ten times to ensure homogeneity. The buttons were homogenized at 1400°C for 100h and then slowly cooled (~1°C/min.). Specimens were then sectioned using an electro-discharge machine (EDM) and mechanically polished for microstructural analysis. The as-cast and annealed samples were viewed in an optical microscope, showing that they are single phase alloys having grain size of 20 μm. The phase of the specimen was verified using x-ray powder diffraction (XRD). For the elastic constant measurements, the polycrystalline C15 $NbCr_2$ specimen was cut into a rectangular parallelepiped with dimensions a=2.660 mm, b=2.405 mm, and c=2.390 mm. The mass-density of the specimen determined from its dimensions and mass was 7.5 g/cm^3, which is 2.6 % lower than the theoretical value (7.7 g/cm^3). In RUS measurement, we have studied 36 resonance peaks at room temperature. A portion of resonant-frequency spectrum of C15 $NbCr_2$ is shown in Fig. 2. The r.m.s. error for the fitting of all 36 resonance peaks in the range from 0.5 MHz to 1.5 MHz is about 0.43%, which indicates a very good agreement between the measured and calculated resonances.

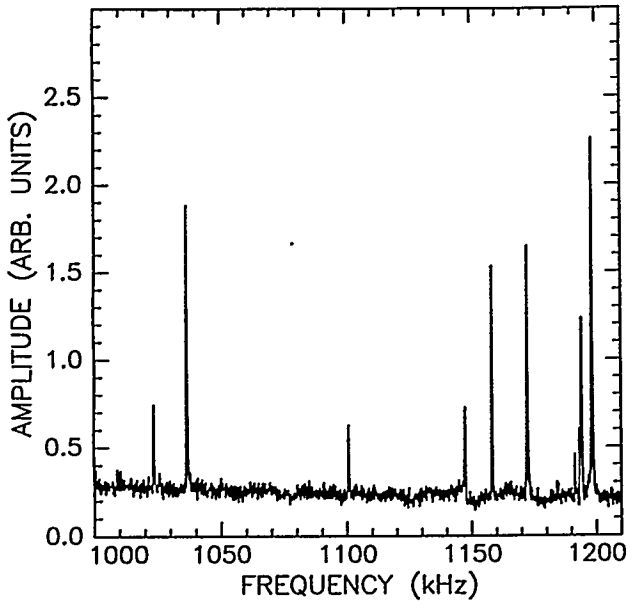

Figure 2: A portion of room temperature resonant-frequency spectrum of C15 $NbCr_2$ [Ref. (12)].

At room temperature, c_{11} and c_{44} of the C15 alloy were determined to be 335.59±2.48 GPa and 79.62±0.02 GPa, respectively. The measured isotropic elastic moduli and Poisson's ratio as calculated from Eqs. (2-5) for the C15 $NbCr_2$ are B=229.4 GPa, E=214.1 GPa, G=79.6 GPa, and ν=0.34, respectively. Two measurements made on two different samples yielded almost the same results.

The present measured bulk modulus is close to, but 8 % smaller than the calculated value (B=250.0 GPa) based on first-principle total energy and electronic structure calculations (31). The error is reasonable because these calculations give the zero-temperature properties and the elastic moduli of the compounds decrease 5-10% as the temperature increases to ambient temperature. The present measured Young's modulus is basically the same as a previously published value (E=219 GPa) (32).

In polycrystals, the Poisson's ratio is bounded in practice by 0 and 1/2. A typical value for materials is 1/3, with 0.28 to 0.42 being the observed range for most materials. The Poisson's ratio is associated with the volume change during uniaxial deformation. If ν is 1/2, no volume change occurs during elastic deformation. In addition, Poisson's ratio provides more information about the characteristic of the bonding forces than any of the other elastic coefficients. It has been proved that ν=0.25 is a lower limit for central-force materials and that ν=0.5 is the upper limit, which corresponds to infinite elastic anisotropy. The Poisson's ratio ν=0.34 (between 0.25 and 0.5) of the C15 $NbCr_2$ indicates that the interatomic forces in the compound are central. In fact, the electronic charge density plots obtained from first-principle calculations for the C15 $NbCr_2$ show, indeed, that there is no substantial directional bonding in the C15 $NbCr_2$ compound (33).

HfV_2+Nb

Based on the Hf-V-Nb ternary phase diagram (34), single phase C15 alloy of composition $Hf_{25}V_{60}Nb_{15}$ was selected for this study. The arc-melted buttons were made in an argon atmosphere using Hf, V, Nb with nominal purities of 99.99 at.%, 99.9 at.% and 99.7 at.%, respectively. The buttons were turned over and remelted five times to ensure homogeneity. The buttons were homogenized at 1250°C for 120 h and then argon quenched. Specimens were then sectioned using an electro-discharge machine (EDM) and mechanically polished for microstructural analysis.

The as-cast and annealed samples were viewed in a scanning electron microscope (SEM) to study the microstructures. The phase of the specimen was verified using x-ray powder diffraction (XRD).

For the elastic constant measurements, the polycrystalline $Hf_{25}V_{60}Nb_{15}$ specimen was cut into a rectangular parallelepiped with dimensions a=2.086 mm, b=1.886 mm, and c=1.449 mm. The mass-density of the specimen was determined from its dimensions and mass. The measured mass-density of the annealed polycrystalline $Hf_{25}V_{60}Nb_{15}$ is 8.613 $g \cdot cm^{-3}$, which is just 1.8 % lower than the theoretical value (8.777 $g \cdot cm^{-3}$). In the determination of the elastic properties of the C15 alloy, RUS measurement was carried out from 70K to room temperature to obtain 36 resonances from 0.35 to 1.2 MHz. A portion of the room temperature RUS spectrum is shown in Fig. 3. The r.m.s. error for the fitting of all 36 resonance peaks is about 0.2%, which indicates a very good agreement between the measured and calculated resonances.

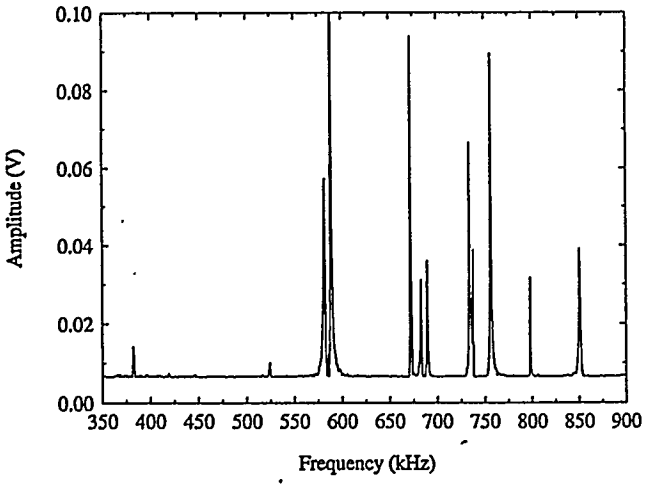

Figure 3: A portion of room temperature resonant-frequency spectrum of C15 $Hf_{25}V_{60}Nb_{15}$ [Ref. (11)].

At room temperature, c_{11} and c_{44} of the C15 alloy were determined to be 189.20±2.48 GPa and 30.07±0.02 GPa, respectively. The measured isotropic elastic moduli and the Poisson's ratio as calculated from Eqs. (2-5) are G=30.1 GPa, E=84.4 GPa, B=146.1 GPa, and ν=0.401, respectively. It is worthwhile to notice that the room temperature elastic properties of the C15 intermetallics are abnormal, i.e., its shear modulus is very low and its Poisson's ratio is above 0.4.

The temperature dependence of the elastic parameters (G, E, B, and ν) of C15 is shown in Fig. 4. Figure 4 indicates the elastic property anomalies of C15 Laves phase: G and E increase with increasing temperature, while ν decreases with increasing temperature, which are opposite to the trends in most solid materials (34).

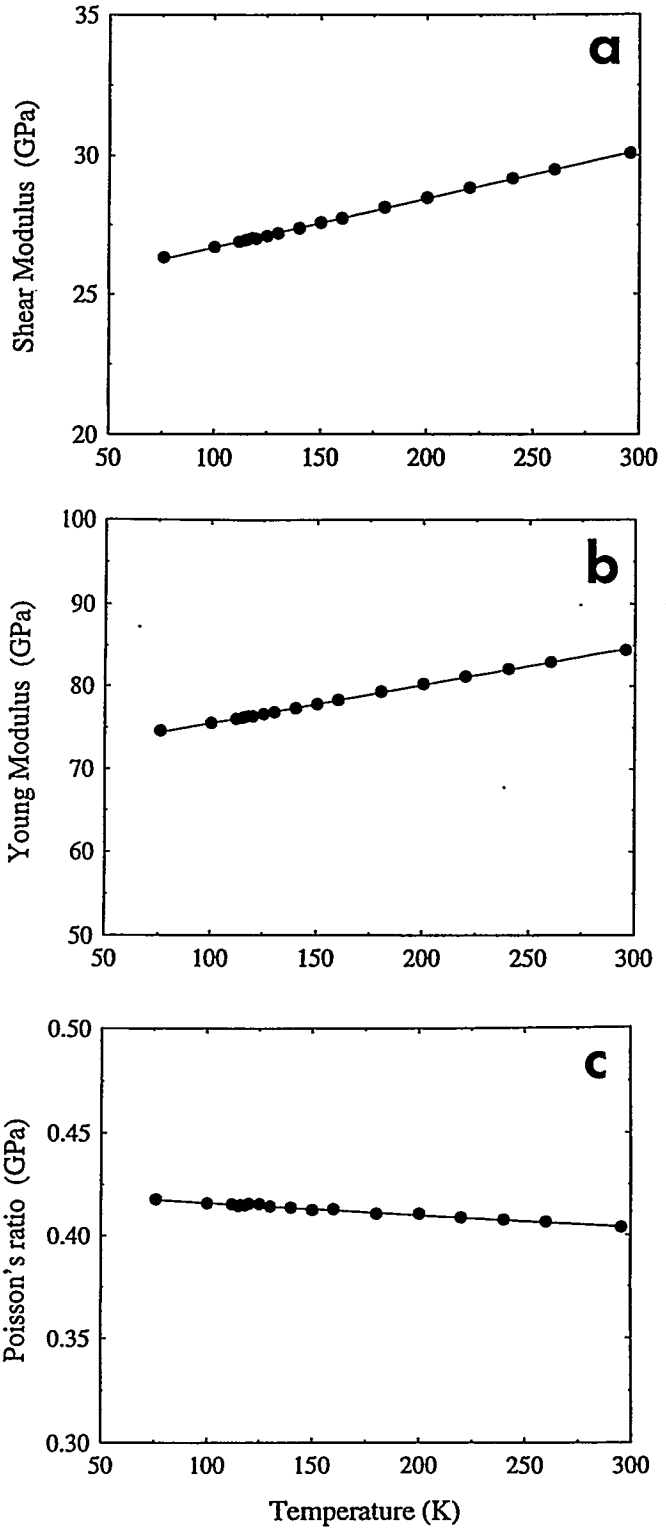

Figure 4: Temperature dependence of elastic constants of C15 $Hf_{25}V_{60}Nb_{15}$: (a) shear modulus G vs T, (b) Young's modulus E vs T, and (c) Poisson's ratio ν vs T [Ref. (11)].

Comparison

Using the measured elastic parameters from RUS for C15 $NbCr_2$ and $Hf_{25}V_{60}Nb_{15}$, we can make the following comparison.

It can be seen from Table I that the room temperature elastic parameters of the two Laves phases are quite different. $NbCr_2$ has relatively high elastic moduli (G, E, and B), while $Hf_{25}V_{60}Nb_{15}$ has very low elastic moduli, comparing general intermetallic phases. Especially, $Hf_{25}V_{60}Nb_{15}$ has extremely low shear modulus, even lower that those of Cu and Au and slightly higher than that of Al. On the other hand, both C15 phases have relatively high Poisson's ratio (>1/3), which are substantially higher than those of most high temperature structural intermetallics. This indicates that the inetratomic bonding in these Laves phases are less-directional, which may have influence on the mechanical properties and deformation behavior of these materials.

Table I Room Temperature Elastic Parameters of C15 $NbCr_2$ and $Hf_{25}V_{60}Nb_{15}$.

Materials	G(GPa)	E(GPa)	B(GPa)	ν
$NbCr_2$	79.6	214.1	229.4	0.34
$Hf_{25}V_{60}Nb_{15}$	30.1	84.4	146.1	0.40

For the temperature dependence of elastic properties, C15 $Hf_{25}V_{60}Nb_{15}$ shows anomalies, which is not commonly-seen in high temperature structural intermetallics. It is suggested that the elastic anomalies in the C15 alloy are related to its electronic structure (35, 36). Based on the same argument, on the other hand, the total energy and electronic structure calculations of C15 $NbCr_2$ (31) suggests that the temperature dependence of the elastic properties of C15 $NbCr_2$ should be normal. The experimental study is currently underway.

Elastic Properties of Titanium Aluminides

TiAl and Ti_3Al

In titanium aluminides, the elastic properties of TiAl and Ti_3Al have been studied in both experiments and theoretical calculations (13, 37, 38). The aggregated isotropic elastic parameters of the two intermetallics are listed in Table II. It can be seen from Table II that the values of isotropic elastic moduli (G, E, and B) of the two titanium aluminides are normal and close. The Poisson's ratios of TiAl and Ti_3Al are very low, much lower that those of most materials (1/3), indicating that the interatomic bonding in these materials are strong directional.

Table II Room Temperature Isotropic Elastic Parameters for TiAl and Ti_3Al.

Materials	G(GPa)	E(GPa)	B(GPa)	ν
TiAl	74	181	110	0.23
Ti_3Al	57	146	106	0.27

O-Phase in Ti-Al-Nb Alloys

Elemental Ti, Al-Nb alloy, Al shots and Nb powder were used for the preparation of O phase alloys by arc-melting (14). The alloys were melted 6-7 times under argon atmosphere in a non-consumable vacuum arc melting furnace. The samples were heat-treated at 1200 °C for 45 minutes, air cooled and annealed at 900 °C for 100-200 hours and water quenched. All the specimens in the as-heat-treated condition showed a single-phase micorstructure with an average grain size in the range 160-200 μm. The chemical compositions of the O phase alloys for the RUS study are tabulated in Table III.

Table III Chemical Composition of the O Phase in Ti-Al-Nb Alloys.

Samples	Chemical Compositions
1	Ti-27Al-20Nb
2	Ti-27Al-24Nb
3	Ti-27Al-20Nb-1Mo
4	Ti-27Al-20Nb-0.5Si
5	Ti-27Al-20Nb-1V
6	Ti-27Al-20Nb-1Zr
7	Ti-27Al-20Nb-1Ta

The room temperature isotropic elastic parameters of the polycrystalline O phase in Ti-Al-Nb alloys were determined using RUS technique. Figure 5 shows a portion of the resonant frequency spectrum for the Ti-27Al-20Nb alloy from 0.7 MHz to 1.0 MHz at room temperature. For this study, a total of 30 observed resonances from RUS were employed to fit the elastic constants of the O phase alloys. The data fitting for the resonances of the seven O phase alloys based on Ti-27Al-20Nb where F reaches a minimum indicates that the r.m.s. error is within 0.16% to 0.6%, which indicates excellent agreement between the measured and calculated resonances. The isotropic elastic parameters of the seven O phase alloys are listed in Table IV. It can be seen from Table IV that the seven O phase alloys based on Ti-27Al-20Nb in general have relatively low shear modulus and normal Poisson's ratio (~1/3) (except for the Si avd V doped alloys). In addition, alloying Ti-27Al-20Nb with Si and transition metal elements does not change the isotropic elastic properties substantially.

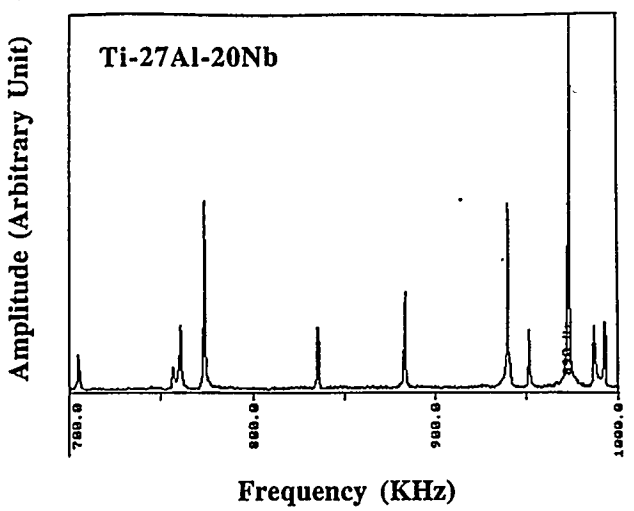

Figure 5: A portion of room temperature resonant-frequency spectrum of the O phase Ti-27Al-20Nb [Ref. (14)].

Table IV Room Temperature Isotropic Elastic Parameters of the Seven O Phase Alloys based on Ti-27Al-20Nb.

Samples	G(GPa)	E(GPa)	K(GPa)	ν
1	48.83	128.78	118.40	0.32
2	51.63	135.90	123.04	0.32
3	50.83	134.08	123.45	0.32
4	53.05	133.50	92.00	0.26
5	50.47	128.32	93.53	0.27
6	48.84	128.82	118.50	0.32
7	49.26	129.98	119.98	0.32

Comparison

The elastic constants for the O phase alloys based on Ti-27Al-20Nb can be compared with those of titanium aluminides, e.g., TiAl, Ti_3Al, and $TiAl_3$, in Ti-Al system, as tabulated in Table V. It can be seen from Table V that the O phase Ti-27Al-20Nb has lower Young's modulus, indicating that it has weaker interatomic bonding than TiAl, Ti_3Al, and $TiAl_3$. Especially, the O phase Ti-27Al-20Nb has a lower shear modulus and a higher Poisson's ratio than those of TiAl, Ti_3Al, and $TiAl_3$. The typical ν values (~0.3) for the O phase alloys indicate that the interatomic forces in the compound are not strongly directional. Low E and G and high ν values may indicate that the O phase alloys have weaker interatomic bonding and structure ordering and less directional bonding than those of TiAl, Ti_3Al, and $TiAl_3$. This may be one of the reasons why the O phase alloys are more deformable at low temperatures.

Table V Room Temperature Isotropic Elastic Parameters for Ti-27Al-20Nb, TiAl, Ti_3Al, and $TiAl_3$.

Materials	G(GPa)	E(GPa)	B(GPa)	ν
Sample 1	49	129	118	0.32
TiAl	74	181	110	0.23
Ti_3Al	57	146	106	0.27
$TiAl_3$ *	99	232	118	0.17

*: from Ref. (39).

Specific Young's modulus (Young's modulus to density ratio) is an important engineering design parameter for materials in aerospace applications. Figure 6 shows the specific Young's modulus for the O phase alloys based on Ti-27Al-20Nb and the intermetallics in Ti-Al system, compared with the constituent elements. It can be seen that the specific Young's modulus of the O phase alloy is similar to those of Ti and Al and substantially larger than that of Nb. However, the specific Young's modulus of the O phase alloy is substantially smaller than those of TiAl, Ti_3Al, and $TiAl_3$, due to its smaller Young's modulus and larger density.

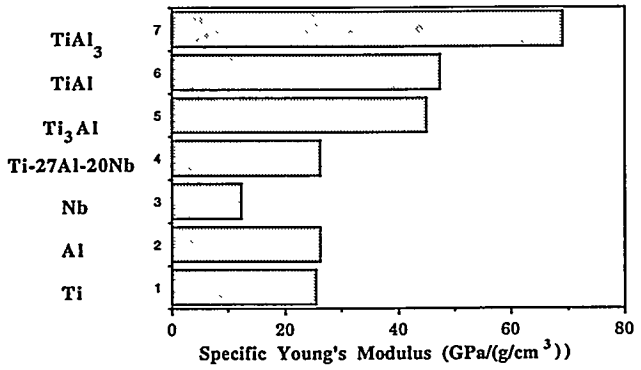

Figure 6: Specific Young's modulus for the O phase Ti-27Al-20Nb, TiAl, Ti_3Al, $TiAl_3$, and the constituent elements.

Elastic Properties of Transition Metal Disilicides

Generally speaking, transition metal disilicide compounds of interest for high temperature structural applications have two crystal structures: the body-centered tetragonal $C11_b$ structure with ···**abab**··· stacking of the {110} planes (e.g. $MoSi_2$ and WSi_2), and the hexagonal C40 structure with ···**abcabc**··· stacking of the equivalent basal planes (e.g. $NbSi_2$, $TaSi_2$, VSi_2, and $CrSi_2$). In addition, $TiSi_2$ has the C54 structure with ···**abcdabcd**··· stacking.

C11$_b$ $MoSi_2$

The room temperature elastic properties of $MoSi_2$ single crystal have been studied by pulse-echo method (40) and RUS (9). RUS measurement on $MoSi_2$ shows that c_{ii} obtained from RUS and the ultrasonic velocity measurement are basically the same (within 1~2% error) and the c_{ij} ($i \neq j$) obtained from RUS are more accurate than those obtained from the ultrasonic velocity measurement.

C40 $NbSi_2$ and $TaSi_2$

In the preparation of C40 $NbSi_2$ and $TaSi_2$ single crystal, powder mixtures of elemental Nb (99 at.%), Ta (99 at.%) and Si (99.99 at.%) were used for the preparation of single crystals of $NbSi_2$ and $TaSi_2$ using the Czochralski technique (15). The as-grown materials were examined using a combination of polarized light microscopy, scanning electron microscopy with x-ray energy dispersive spectroscopy, and transmission electron microscopy. The results revealed that the as-grown materials are single crystals, with no grain boundaries or precipitates. The Laue back reflection x-ray diffraction technique was employed to determine the orientation of the single crystal rods (16).

For elastic constant measurements, the single crystal $NbSi_2$ and $TaSi_2$ specimens were cut into rectangular parallelepipeds with dimensions x_1=1.292±0.002 mm, x_2=1.802±0.003 mm, and x_3=2.494±0.004 mm for $NbSi_2$, and x_1=2.043±0.003 mm, x_2=2.390±0.002 mm, and x_3=2.122±0.003 mm for $TaSi_2$. A set of ground steel shims on a glass plate was used for obtaining an accurate rectangular parallelipiped with precise dimensions from the as-grown oriented single crystals. The Laue back reflection x-ray diffraction technique was used to orient $\mathbf{x}_1$ parallel to $[10\bar{1}0]$, $\mathbf{x}_2$ parallel to $[\bar{1}2\bar{1}0]$, and $\mathbf{x}_3$ parallel to [0001]. The mass-densities of the specimens were determined from their dimensions and masses.

Figure 7 shows a portion of the resonant frequency spectrum for single crystal $NbSi_2$ from 1.7MHz to 2.5MHz and a portion of the resonant frequency spectrum for single crystal $TaSi_2$ from 0.9 MHz to 1.2 MHz at room temperature. The accuracy of the frequency measurements was about 30 ppm. For this study, a total of 33 observed resonances from RUS were employed to fit the elastic constants of the $NbSi_2$ and $TaSi_2$ single crystals. The data fitting for the resonances of $NbSi_2$ and $TaSi_2$ where the F reaches a minimum indicates that the r.m.s. errors are 0.24% for $NbSi_2$ and 0.29% for $TaSi_2$, which show excellent agreement between the measured and calculated resonances. The elastic stiffness constants at room temperature obtained from these fittings are tabulated in Table VI.

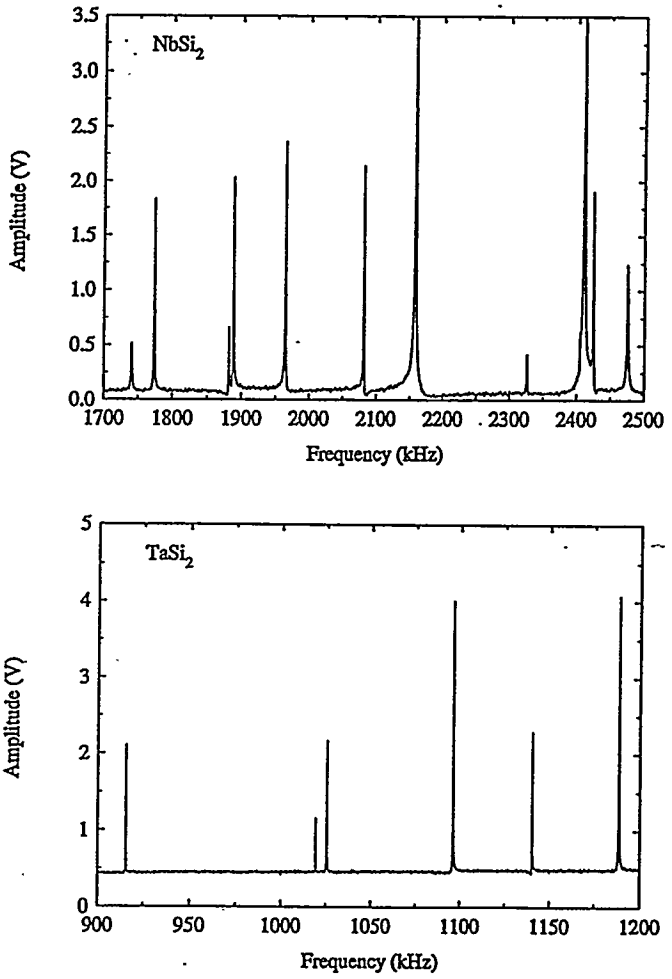

Figure 7: Room temperature resonant-frequency spectra of single crystal specimens: (a) $NbSi_2$ and (b) $TaSi_2$, [Ref. (16)].

Table VI Room Temperature Single Crystal Elastic Constants of C40 $NbSi_2$ and $TaSi_2$.

c_{ij} (GPa)	$NbSi_2$	$TaSi_2$
c_{11}	384.0	375.3
c_{33}	473.5	476.7
c_{44}	146.8	143.7
c_{12}	75.9	78.4
c_{13}	87.6	90.1

c_{11} and c_{33} are important elastic constants which are related to the deformation behavior, atomic bonding characteristics, and melting temperature. It can be seen from Table VI that $c_{33} > c_{11}$ for the C40

compounds. This is also true for the $C11_b$ transition metal disilicides. Its implication is that the atomic bonds along [0001] between nearest neighbors are stronger than those along any directions in the basal plane. In addition, the ratio of c_{33} to c_{11} for C40 $NbSi_2$, and $TaSi_2$ is about 1.2, and the ratio of the atomic distance in the $[10\bar{1}0]$ direction to the average atomic distance in the [0001] direction for these C40 compounds is also close to 1.2. The same trend holds true for other transition metal disilicides, e.g. $C11_b$ $MoSi_2$ and WSi_2 (40). In the $C11_b$ compounds, the ratio of the atomic distance in the [100] direction to an average atomic distance in the [001] direction is approximately equal to the c_{33}/c_{11} ratio of these compounds. Nakamura et al. (40) suggest that these two ratios are closely related to each other, because the elastic constants are closely related to the interatomic potential energies.

The Cauchy relations between elastic stiffness constants for hexagonal crystals with central forces are:

$$c_{13}=c_{44},\ c_{11}=3c_{12}\ (\text{or } c_{12}=c_{66}) \quad (6)$$

It can be seen from Table VI that the Cauchy relations do not hold true for the C40 transition metal disilicides by more than a factor of 2-3, and this fact implies that the interatomic forces in these compounds are non-central. This may have a substantial influence on the dislocation core structure and mechanical behavior of these materials.

The room temperature isotropic elastic constants of polycrystalline $NbSi_2$ and $TaSi_2$ are shown in Table VII.

Table II Room Temperature Isotropic Elastic Constants of $NbSi_2$ and $TaSi_2$.

Materials	G (GPa)	E (GPa)	B (GPa)	ν
$NbSi_2$	153.2	362.8	191.5	0.18
$TaSi_2$	151.0	359.0	192.5	0.19

The bulk, shear and Young's moduli of the C40 materials are substantially higher than those of the constituent elements and the average value based on the rule of mixtures. The large elastic moduli of the C40 materials are due to stronger interatomic bonding and high structure ordering. On the other hand, the Poisson's ratios of the C40 materials are much smaller than those of the constituent elements and the average value based on the rule of mixtures. The low ν values (substantially smaller than 0.25) for the C40 materials indicate again that the interatomic forces in the compound are non-central.

Comparison

It is worthwhile comparing the elastic properties of hexagonal C40 disilicides and tetragonal $C11_b$ disilicides, because this may give us some insights and prediction for their mechanical behavior.

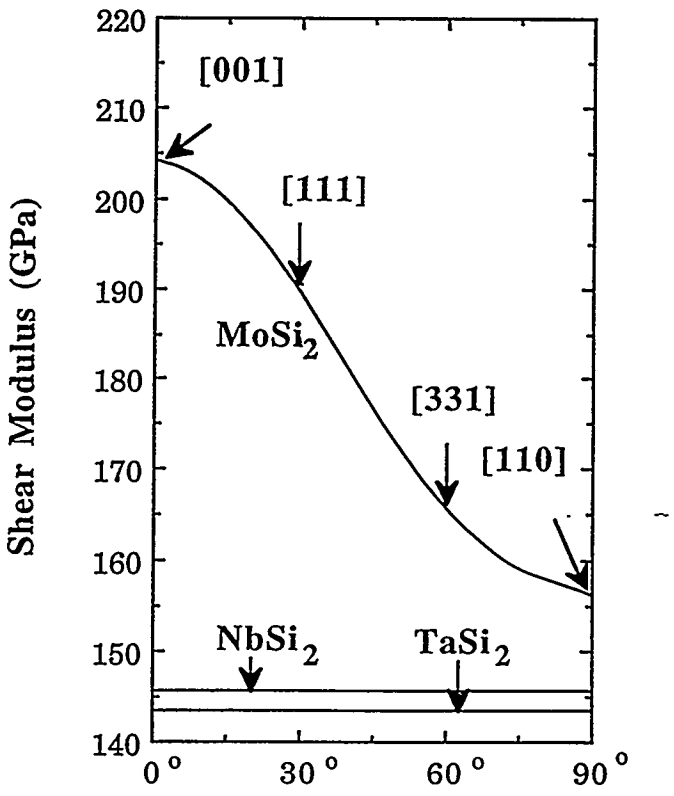

Figure 8: Orientation dependence of shear modulus on the $(1\bar{1}0)$ shear plane for $C11_b$ $MoSi_2$. The direction of shear is rotated on the shear plane from [001] to [110] (Compiled from the data in Ref. (40)). The horizontal lines are the shear moduli on the {0001} plane for the C40 MSi_2 (M=Nb and Ta). The direction of shear stress is rotated on the shear plane from $[10\bar{1}0]$ to $[\bar{1}2\bar{1}0]$.

Among the c_{ij}, c_{44} is relevant for considering the mechanical properties of these materials because it is related to the shear behavior on the {0001} plane for C40 compounds and the {001} plane for $C11_b$ compounds. The c_{44} values of C40 $NbSi_2$ and $TaSi_2$ are substantially smaller that those of $C11_b$ $MoSi_2$. Therefore it might be expected that the corresponding shear deformation could occur more easily in these C40 compounds than in $C11_b$ $MoSi_2$. More importantly, c_{44} of the C40 compounds should be compared with the shear modulus on the pseudo-hexagonal close-packed {110} planes of $C11_b$ $MoSi_2$, which is dependent on the shear direction.

For example, the shear modulus on the {110} plane in the [001] direction is $c_{66}=(c_{11}-c_{12})/2$, but this is still substantially higher for the $C11_b$ compounds (15). The elastic anisotropy of the transition metal disilicides has an important impact on the mechanical properties of the systems, especially on dislocation structures and mechanisms. Comparing the shear moduli on the close-packed planes for the C40 compounds and $C11_b$ $MoSi_2$, we find that the shear moduli on the {0001} plane for C40 $NbSi_2$ and $TaSi_2$ are substantially lower than those on the {110} plane for the $C11_b$ $MoSi_2$, as shown in Fig. 8. This may be related to the low temperature ductility carried out by basal slip in C40 $NbSi_2$ and $TaSi_2$ single crystals (41).

Summary

A novel nondestructive evaluation method, resonant ultrasound spectroscopy (RUS), is reviewed with an emphasis upon defining the elastic properties of intermetallic phases. We have used this method to measure the elastic properties of high temperature structural imtermetallic phases, e.g. Laves phases, titanium aluminides, and transition metal disilicides.

For C15 Laves phases $NbCr_2$ and HfV_2+Nb, the isotropic elastic parameters have been obtained. $NbCr_2$ has normal elastic behavior, while HfV_2+Nb has elastic anomalies, e.g., very low shear modulus and anomalous temperature dependence of elastic parameters. However, for both of them, the Poisson's ratios are relatively high (>1/3), indicating that the interatomic bonding in these systems may not be strong directional.

For the O phase in Ti-Al-Nb alloys, the isotropic elastic parameters of seven O phases based on Ti-27Al-20Nb have been measured. They have relatively low shear modulus (~50 GPa) and normal Poisson's ratio (~1/3). The specific Young's modulus of the O phase in Ti-Al-Nb alloys is close to those of Ti and Al. Alloying the O phase alloys with Si and transition metal elements does not change the isotropic elastic moduli substantially.

For the C40 transition metal disilicides, $NbSi_2$ and $TaSi_2$, the single crystal elastic constants have been obtained. It holds true for the C40 transition metal disilicides that $c_{11}>c_{44}$, $c_{33}>c_{66}$, and $c_{33}>c_{11}$, as for the $C11_b$ transition metal disilicides, e.g., $MoSi_2$. This is associated with the characteristics of the interatomic bonding in the compounds. It also holds true that $c_{33}/c_{11}\approx 1.2$, as for the $C11_b$ $MoSi_2$. This is due to the fact that the elastic constants are closely related to the interatomic potential energies. The shear moduli of $NbSi_2$ and $TaSi_2$ single crystals, are relatively low on the basal plane, compared with that on the pseudo-hexagonal close-packed {110} plane of $C11_b$ $MoSi_2$. This may be one of the reasons for the low temperature deformability of $NbSi_2$ and $TaSi_2$ via basal dislocation slip. The bulk, shear and Young's moduli of C40 $NbSi_2$ and $TaSi_2$ are much higher than those of the constituent elements. The Poisson's ratios of the C40 $NbSi_2$ and $TaSi_2$ are 0.18 and 0.19, respectively, which are substantially smaller than those of the constituent elements (in fact those of most materials), but higher than those of $C11_b$ $MoSi_2$. This means that the interatomic forces in the C40 compounds are non-central, but less-directional than those of $MoSi_2$.

Acknowledgment

This work has been supported under the auspices of the United States Department of Energy, Office of Basic Energy Science and Los Alamos National Laboratory Directed Research and Development (LDRD) project. F. Chu and Y. He thank A. Migliori, Ming Lei, T. Darling, and Y.-M. Liu for many useful discussions and comments.

References

1. A. Migliori, J. L. Sarro, W. M. Visscher, T. M. Bell, Ming Lei, Z. Fisk, R. G. Leisure, Physica B, 1993, 1-24.
2. A. Migliori and Z. Fisk, Los Alamos Science, 1993, Vol. 21, 182-194.
3. J. Maynard, Physics Today, January, 1996, 26-31.
4. V. T. Kuokklar and R. B. Schwarz, Rev. Sci. Instrum. 1992, Vol. 63, 3136-3139.
5. D. B. Frasher and R. C. LeCraw, Rev. Sci. Instrum., 1964, Vol. 35, 1113.
6. N. Soga and O. L. Anderson, J. Geophysics, 1967, Vol. 72, 1733.
7. H. H. Demarest, J. Acoust. Soc. Am. 1971, Vol. 49, 768.
8. I. Ohno, J. Phys. Earth, 1976, Vol. 24, 355.
9. Y. He, F. Chu, R. B. Schwarz, T. Darling, and J. D. Embury, In preparation.
10. B. A. Auld, Acoustic Fields and Waves in Solids, Vol. I, (New York, NY: John Wiley, 1973).
11. F. Chu, Ming Lei, A. Migliori, S. P. Chen, and, T. E. Mitchell, Phil. Mag. B., 1994, Vol. 70, 867-880.
12. F. Chu, Y. He, D. J. Thoma, and T. E. Mitchell, Scripta Met. et Mater., 1995, Vol. 33, 1295-1300.
13. Y. He, R. B. Schwarz, A. Migliori, and S. H. Whang, J. Mater. Res., 1995, Vol. 10, 1187-1195.

14. F. Chu, T. E. Mitchell, B. Majumdar, D. Miracle, T. K. Nandy, and D. Banerjee, submitted to Intermetallics.
15. F. Chu, Ming Lei, S. A. Maloy, T. E. Mitchell, A. Migliori, and J. Garrett, Phil. Mag. B., 1995, Vol. 71, 373-382.
16. F. Chu, Ming Lei, S. A. Maloy, J. J. Petrovic, and T. E. Mitchell, Acta Met. et Mater. 1996, In press.
17. J. D. Maynard, J. Acoust. Soc. Am., 1992, Vol. 91, 1754.
18. W. M. Visscher, Los Alamos Report, 1991, LA-UR-91-2884.
19 W. H. Press, B. P. Flannery, S. A. Teukolsky, and W. T. Vetterling, in Numerical Receipt, (Cambridge, UK: Cambridge University Press, 1986) 215.
20. J. F. Nye, Physical Properties of Crystals, (London, UK: Oxford University Press, 1979).
21. P. S. Spoor, J. D. Maynard, and A. R. Kortan, Phys. Rev. Lett., 1995, Vol. 75, 3462-3465.
22. D. J. Thoma and J. H. Perepeako, Mater. Scien. Eng. A., 1992, Vol. 156, 97.
23. J. D. Livingston and E. L. Hall, J. Mater. Res., 1990, Vol. 5, 5.
24. F. Chu and D. P. Pope, Mater. Sci. Eng. A., 1993, Vol. 170, 39-47.
25. D. Banerjee, Phil. Mag. A., 1995, Vol. 72, 1559.
26. R. G. Rowe, US Patent No. 5032357 , 1991.
27. T. E. Mitchell, R. G. Castro, J. J. Petrovic, S. A. Maloy, O. Unal, and M. M. Chadwick, Mater. Sci. Eng. A., 1992, Vol. 155, 241.
28. J. J. Petrovic, MRS Bulletin, 1993, Vol. XVIII, No. 7, 35.
29. K. Ito, H. Inui, Y. Shirai, and M. Yamaguchi, Phil. Mag. A., 1995, Vol. 72, 1075-1097.
30. Y. Umakoshi, T. Nakashima, T. Nakano, and E. Yanagisawa, in High Temeprature Silicides and Refractory Alloys, ed. by C. L Briant, J. J. Petrovic, B. P. Bewlay, A. K. Vasudevan, and H. A. Lipsitt, MRS Symp. Proc. Vol. 322, (Pittsburgh, PA: MRS, 1994), 9.
31. F. Chu, D. J. Thoma, Y. He, T. E. Mitchell, S. P. Chen, and J. H. Perepezko, in High Temperature Intermetallic Alloys IV, ed. by J. Horton, I. Baker, S. Hanada, and R. D. Noebe, MRS Symp. Proc. Vol. 364 (Pittsburgh, PA: MRS, 1995), 1089.
32. U. Kramer and G. E. R Schulze, Kristall und Technik, 1968, Vol. 3, 417.
33. A. H. Ormeci, F. Chu, J. M. Wills, T. E. Mitchell, S. P. Chen, R. C. Albers, and D. J. Thoma, submitted to Phys. Rev. B.
34. H. M. Ledbetter, in Materials at Low Temperatures, ed. by R. P. Reed and A. F. Clark, (Metals Park, OH: ASM, 1983), 1-45.
35. S. V. Vonsovsky, Y. A. Izyumov, and E. Z. Kurmaev, Sperconductivity of Transition Metals, (Berlin, Springer, 1982).
36. F. Chu, M. Sob, R. Siegl, T. E. Mitchell, D. P. Pope, and S. P. Chen, Phil. Mag. B., 1994, Vol. 70, 881-892.
37. C. L. Fu and M. H. Yoo, Phil. Mag. A., 1990, Vol. 62, 159-165.
38. C. L. Fu, J. Zou, and M. H. Yoo, Scripta. Met. et Mater., 1995, Vol. 33, 885-891.
39. C. L. Fu and M. H. Yoo, Mater. Chem. Phys., 1992, Vol. 32, 25.
40. M. Nakamura, S. Matsumoto, and T. Hirano, J. Mater. Sci., 1990, Vol. 25, 3309.
41. Y. Umakoshi, T. Nakashima, T. Nakano, and E. Yanagisawa, in High Temperature Silicides and Refractory Alloys, ed. by C. L. Briant, J. J. Petrovic, B. P. Bewlay, A. K. Vasudevan, and H. A. Lipsitt, MRS Symp. Proc. Vol. 322, (Pittsburgh, PA: MRS, 1994), 9.